Mechanics of Advanced Composite Structures 6 (2019) 27–34

Semnan University

Mechanics of Advanced Composite Structures

journal homepage: http://MACS.journals.semnan.ac.ir

Nonlinear Vibration Analysis of the Composite Cable using Perturbation Method and the Green-Lagrangian Nonlinear Strain

R. Khodabakhsh*, M.R. Dashtbayazi

Department of Mechanical Engineering, Faculty of Engineering, Shahid Bahonar University of Kerman, Kerman, Postcode 7618868366, Iran

PAPER INFO

Paper history:
Received 2018-10-15
Received in revised form 2019-02-21
Accepted 2019-04-26

Keywords:
Nonlinear vibration
Cable
Composite
Nonlinear strain

ABSTRACT

In this study, nonlinear vibration of a composite cable is investigated by considering nonlinear stress-strain relations. The composite cable is composed of an aluminum wire as reinforcement and a rubber coating as matrix. The nonlinear governing equations of motion are derived about to an initial curve and based on the fundamentals of continuum mechanics and the nonlinear Green-Lagrangian strain, using the Hamilton's principle. The equations of motion of the system are reduced into the ordinary differential equations using the Galerkin method, and solved by the perturbation method (multiple scales). Time-response diagrams are presented for the composite cable with different volume fractions of the matrix and the reinforcement. It is predicted that the more volume fraction of the matrix is, the more nonlinear quadratic and cubic terms in the governing equations of motion affects the vibration of the cable. Results indicate that increasing the length of the cable would decrease the amplitude of the time response of the system.

1. Introduction

Cables play an important role in the various applications, such as mechanical, civil and electrical engineering. Since, the cables are used in numerous engineering applications, vibrational behavior of them have been extensively studied by the researchers.

A major material of the cables used in different applications is composite which consists of two or more than two parts such as metal and rubber. The metal acts as a conductor or reinforcement and rubber is as protector or matrix. So, this makes the study of vibrations of this engineering structure a great importance.

The cables are subjected to tention and are very deformable. This is one of the reasons that the cables have nonlinear vibration. The nonlinear vibration introduces cubic nonlinear terms to the equations of motion [1]. On the other hand, an intial curvature of the cables adds quadratic nonlinear terms to the equations of motion and the nonlinear terms significantly affect the vibrational behavior of the system.

Studying the nonlinear vibrations of the cables and also composite structures has been of great interest in recent years by many researchers. Rega and Srinil have investigated the nonlinear hybrid-mode resonant forced oscillations of sagged inclined cables at avoidances. They conclude that the chaotic dynamics were endowed with remarkable asymmetry of spatially nonuniform, strongly time-varying, tensile/compressive oscillation-induced tensions [2].

Wang and Zhao [3] have analized the nonlinear planar dynamics of suspended cables by the continuation technique. They observed that sag-to-span ratio of the cable plays a significant role in the drift of the frequency-response curves and the effect of the quadratic non-linearity. Also, the amplitudes

* Corresponding author. Tel.: +98-34-32111763; Fax: +98-34-32120964
E-mail address: dashtbayazi@uk.ac.ir

DOI: 10.22075/MACS.2019.16187.1169

of the non-linear response are related to the sag-to-span ratio of the cable.

Transverse vibration of nonlinear strings has been modeled by Chen and Ding [4]. They concluded that the errors of the two models are both relatively small even for reasonable large vibration amplitude, the model errors increase with the vibration amplitude and the Kirchhoff string equation yields better results. Chen et al. [5] have investigated the nonlinear dynamics for transverse motion of axially moving strings. They summarized latest progress on nonlinear dynamics for transverse motion of axially moving strings and presented a uniform governing equation incorporated arbitrary forms of the constitutive law of the string material. Rega [6] have studied the theoretical and experimental nonlinear vibrations of sagged elastic cables.

Salehi Ahmad Abad et al. [7] have performed a nonlinear analysis of cable structures under general loadings. The acceptable convergence of the proposed models in their research, simplicity and direct equations reflect their capability, found through making comparison with other models, in analyzing some given numerical examples. Nonlinear response of elastic cables with flextural-torsional stiffness has been analized by Arena et al. [8]. Their work presented a fully nonlinear model of cables based on the special Cosserat theory of rods. As such, the model conceives the elastic cable as a very slender rod that suffers extension, bending, shear and twist. It was shown that the initial prestress state of the cable drives differently the onset of the boundary layers, the stress peaks within them and their spatial extension. Yashavanta Kumar and Satish Kumar [9] have studied free vibration of smart composite beams. The modal analysis of the smart cantilever beam was performed using the ANSYS s to reveal the fundamental modal frequencies and modal shapes.

Kumar et al. [10] studied the nonlinear bending and vibration analysis of quadrilateral composite plates. Piraccini and Sante [11] measured the nonlinear vibration response in aerospace composite blades using pulsed air flow excitation. Nonlinear vibration of sandwich plates with FG-GRC face sheets in thermal environments was studied by Wang and Shen [12]. They discussed in details the effects of distribution type of reinforcements, core to face sheet thickness ratio, temperature variation, foundation stiffness and in plane boundary conditions on the nonlinear vibration characteristics of sandwich plates with piece-wise functionally graded GRC face sheets. Mao and Zhang [13] investigated the linear and nonlinear free and forced vibrations of graphene reinforced piezoelectric composite plate under external voltage excitation. They used Halpin Tsai's parallel model to predict the effective Young's Modulus and the effective mass density, poisson's ratio and piezoelectric properties were calculated by the rule of mixture. Governing equations of motion were derived based on the first-order shear deformation plate theory, Von Karman nonlinear geometric relationship and Hamilton's principle. Zhang et al. [14] analysed the nonlinear vibrations near internal resonances of a composite laminated piezoelectric rectangular plate. Using Reddy's third order shear deformation plate theory and Hamilton's principle, the nonlinear governing equations of motion were derived. The influences of the transverse, in-plane and piezoelectric excitations on the bifurcations and chaotic behaviors of the composite laminated piezoelectric laminated rectangular plate were investigated numerically. Sheng and Wang [15] studied the nonlinear vibration of FG beams subjected to parametric and external excitations. In their study, nonlinear frequency-response of FG beams was investigated using the method of multiple scales. Nonlinear free vibration of bi-directional functionally graded beams was discussed by Tang et al. [16]. They presented a novel model of Euler-Bernoulli beams made of bi-directional (2D) functionally graded materials to study the nonlinear free vibration. They found that nonlinear dynamic properties are highly dependent on materials properties and also the numerical examples in this research show the influences of various physical parameters, such as the material FG indeices, on the dimensionless nonlinear frequency of the 2D FG beam. Wang et al. [17] investigated the vibration response of a functionally graded graphene nanoplatelet reinforced composite beam under two successive moving masses. They used a modified Halpin-Tsai micromechanics model to evaluate the effective Young's modulus of the beam. This research showed that the geometry of the graphene nanoplatelet plays an important role on the dynamic response of the beam. Fan et al. [18] studied the nonlinear forced vibration of FG-GRC laminated plates resting on visco-Pasternak foundations. The analytical results of this research showed that the FG distribution pattern of graphene, the temperature variation, the foundation stiffness and the damping factor have significant influence on the dynamic responses of FG-GRC laminated plates. Nonlinear vibration of a composite plate to harmonic excitation with initial geometric imperfection in thermal environments was studied by Liu et al. [19]. The effects of the temperature, equivalent in plane boundary stiffness and initial geometric imperfection on the dynamic behavior were investigated through a detail parametric study.

They showed that the critical buckling temperature of a perfect plate decreases with increasing the equivalent in-plane boundary stiffness significantly. Bayat and Ekhteraei Toussi [20] investigated a nonlinear analysis on structural damping of SMA hybrid composite beams. First-order shear deformation beam theory and large deflection Von Karman strain displacement were utilized to obtain the stress field. The governing equation of forced vibration in a beam under transient dynamical loading was developed and discretized using the method of differential-integral quadrature.

The existing literature show that they are all based on simple cables made by single materials. The assumption of elastic cable, makes it simpler to solve the equations of motion and prevents the appearance of nonlinear terms caused by material of the cable, in the equations of motion. Sincecomposite cables are used in various engineering applications, in this article, a two-end clamped composite cable is considered and the effect of composite material on the free vibration of the cable is investigated by considering the nonlinear Green-Lagrangian strain.

2. Problem Formulation

The modeling and vibration of cables are much more complex than strings because of its initial sag. In this reaesrch, the composite cable made of two layers is considered as shown in Fig. 1.

Equivalent elastic modulus and equivalent density of the composite cable along its length are obtained by the rule of the mixtures as [21]:

$$E_{eq} = E_f V_f + E_m V_m \quad (1)$$

$$\rho_{eq} = \rho_f V_f + \rho_m V_m \quad (2)$$

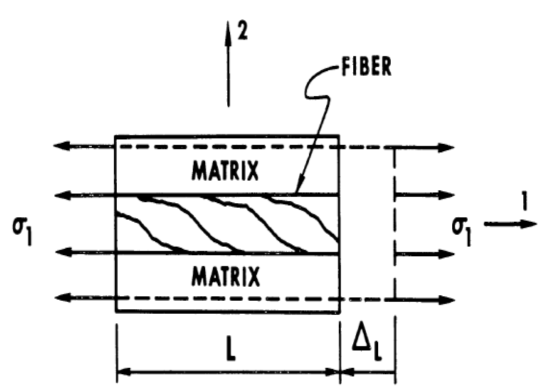

Fig. 1. Two layered composite cable [21].

where E_f, E_m, ρ_f, ρ_m, V_f and V_m are the elastic modulus, the density and the volume fractions of the fiber and the matrix in the composite material of the cable, respectively.

The composite cable is suspended between two fixed supports and deformed configuration of the composite cable and the cartesian coordinate X_1, X_2 are shown in Fig. 2. p_0 is a point that shows position of a particle of the cable when the cable is not loaded. Point $\hat{p}$ indicates the deformed position of p_0 when the cable is under static loads, and point p is the deformed position of p_0 under static and dynamic loads. Coordinates of the $\hat{p}$ and p are considered to be (α_1, α_2) and(x_1, x_2), respectively. S represents the undeformed arclength measured from point M to the place of observed particle at thepoint p_0; $\hat{s}$ denotes deformed arclength under static loads; $\tilde{s}$ represents the deformed arclength under dynamic loads [1].

Dynamic displacements of the p along the x_1 and x_2 axes are indicated by u_1 and u_2, respectively, thus [1]:

$$x_i = \alpha_i + u_i \qquad \text{for } i = 1,2 \quad (3)$$

Considering the nonlinear Green-Lagrangian strain as [22]:

$$\varepsilon_{11} = \frac{(d\tilde{s})^2 - (ds)^2}{2(ds)^2} \quad (4)$$

And applying Eq. (3), the nonlinear strain of the composite cable is given by:

$$\varepsilon_{11} = \alpha_1' u_1' + \alpha_2' u_2' + \frac{1}{2}[(u_1')^2 + (u_2')^2] \quad (5)$$

where $(\,)' \equiv \frac{\partial()}{\partial s}$.

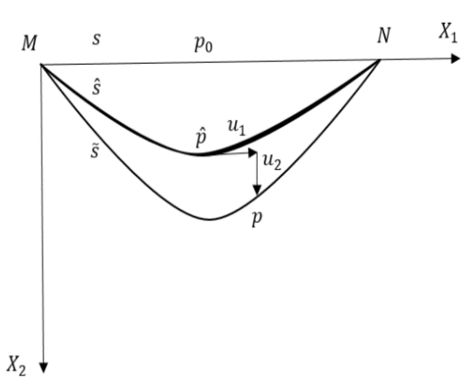

Fig. 2. Deformed configuration of the composite cable.

Assuming the strain energy function of the Saint-Venant Kirchhoff model is [22]:

$$W(\varepsilon) = \frac{\lambda}{2}(\mathrm{tr}\varepsilon)^2 + \mu(\mathrm{tr}\varepsilon^2) \tag{6}$$

where ε is the strain and λ, μ are the Lamme constants, respectively. The second Piola-Kirchhof stress is given by [22]:

$$P = \frac{\partial W(\varepsilon)}{\partial \varepsilon} \tag{7}$$

In order to derive the governing equations of the motion, the Hamilton's principle is used through Eq. (8) as follows [1]:

$$\int_{t_1}^{t_2} (\delta T - \delta \Pi + \delta W_{nc})dt = 0 \tag{8}$$

where δT, $\delta \Pi$ and δW_{nc} are the variations of kinetic, strain and nonconservative energy, respectively. Assuming planar displacement and neglecting horizontal motion of the composite cable, the only nonzero displacement will be u_2, so, the variation of the kinetic energy is obtained as:

$$\delta T = \int_0^L \rho_{eq} A_0 [(\frac{\partial u_2}{\partial t}\frac{\partial(\delta u_2)}{\partial t})]ds \tag{9}$$

where L and A_0 are the length and the initial cross section of the cable. Using Equations (5), (6) and (7), the variation of the strain energy is obtained as follows:

$$\delta \Pi = \int_0^L P_{11} A_0 [(\frac{\partial \alpha_2}{\partial s} + \frac{\partial u_2}{\partial s})(\frac{\partial(\delta u_2)}{\partial s})]ds \tag{10}$$

In Eq. (10), P_{11} is the second Piola-Kirchhof stress in the axial direction of the cable. The variations of the non-conservative energy in the Hamilton's principle is calculated as follows [1]:

$$\delta W_{nc} = \int_0^L (f_2 \delta u_2)ds \tag{11}$$

where f_2 is the sumation of $\widehat{f_2}$ and $\widetilde{f_2}$ that represent static and dynamic loads. Substituting equations (9), (10) and (11) in equation (8) and integrating by parts would give the equation of motion as:

$$\begin{aligned}\rho_{eq} A_0 \ddot{u}_2 = E_{eq} A_0 \Big[&\big(\alpha_2'' u_2' + \alpha_2' u_2''\big)(\alpha_2' + u_2') \\ &+ \alpha_2' u_2' \big(\alpha_2'' + u_2''\big) \\ &+ \big(u_2'' u_2'\big)(\alpha_2' + u_2') \\ &+ \frac{1}{2}\big(\alpha_2'' + u_2''\big)((u_2')^2)\Big] \\ &+ f_2\end{aligned} \tag{12}$$

where E_{eq} in Eq. (12) indicates the equivalent elastic modulus of the composite material of the cable.

Since free vibration of the cable is considered, f_2 will be zero. Statical deformed configuration of the cable is assumed to be:

$$\begin{aligned}\alpha_1(s) &= s \\ \alpha_2(s) &= a\cosh(\frac{s}{a})\end{aligned} \tag{13}$$

where a is a parameter that determines how quickly the catenary opens up, and it is changed between 0.05 and 1. Substituting Eq. (13) in Eq. (12), the equation of the motion becomes:

$$\begin{aligned}\rho_{eq} \ddot{u}_2 = E_{eq} [&\left(\frac{2}{a}\right)\sinh\left(\frac{s}{a}\right)\cosh\left(\frac{s}{a}\right) \\ &+ \left(\frac{1}{a}\right)\cosh\left(\frac{s}{a}\right)u_2' \\ &+ \sin^2 h\left(\frac{s}{a}\right)u_2'' \\ &+ 3\sinh\left(\frac{s}{a}\right)u_2' u_2'' \\ &+ \frac{3}{2}(u_2')^2 u_2'' \\ &+ \left(\frac{1}{2a}\right)\cosh(\frac{s}{a})(u_2')^2]\end{aligned} \tag{14}$$

By considering mode shape o $\varphi(s) = \sin\frac{\pi s}{L} f$ that satisfies boundary condition of the system and applying the Galerkin method, time response equation of the system is given as follows:

$$\ddot{\xi}(t) + \omega_0^2 \xi(t) + k_2 \xi^2(t) + k_3 \xi^3(t) = 0 \tag{15}$$

where

$$\begin{aligned}\omega_0^2 = \left(\frac{Y\pi^3}{4\rho_{eq}L^2}\right)&\left(\frac{a^2\pi\cosh(\frac{2L}{a})}{a^2\pi^2 + 4L^2} + \left(\frac{a^2\pi}{a^2\pi^2 + 4L^2}\right) - \frac{2}{\pi}\right) \\ &+ \left(\frac{\pi^2 E_{eq}}{a^2\pi^2\rho_{eq}L + 4\rho_{eq}L^3}\right)\left(L\cosh\left(\frac{2L}{a}\right)\right. \\ &\left. + aL^2\right) + (\frac{\pi^2 E_{eq}}{2\rho_{eq}L})(\frac{L\sinh(\frac{L}{a})}{a^2\pi^2 + L^2})\end{aligned} \tag{16}$$

$$k_2 = -\left(\frac{3E_{eq}\pi^4}{2\rho_{eq}L^4}\right)\left(\frac{a^2L\pi\sinh\left(\frac{L}{a}\right)}{4a^2\pi^2+L^2}\right) - \left(\frac{E_{eq}\pi^3}{8\rho_{eq}L^3}\right)\left(\frac{L^2\sinh\left(\frac{L}{a}\right)}{4a^2\pi^2+L^2} + \sinh\left(\frac{L}{a}\right)\right) \tag{17}$$

$$k_3 = \frac{E_{eq}\pi^4}{2\rho_{eq}L^4} \tag{18}$$

In Eq. (15), the quadratic and the cubic nonlinear terms are observed and affect the behavior of the system significantly.

3. Perturbation (Multiple Scales) Method

By assuming $= \epsilon q$, where ϵ is a finite and small parameter; and substituting it in Eq. (15), the following equation is obtained [23]:

$$\mathbf{q + \omega_0^2 q + k_2 \epsilon q^2 + k_3 \epsilon^2 q^3 = 0} \tag{19}$$

In order to apply multiple scales method, q is considered to be [23]:

$$\mathbf{q = q_1(T_0, T_1, T_2) + \epsilon q_2(T_0, T_1, T_2) + \epsilon^2 q_3(T_0, T_1, T_2) + o(\epsilon^2 t)} \tag{20}$$

Substituting Eq. (20) into (19) and following the method of multiple scales [13], Eq. (19) leads to lower order linear equations [23]:

$$\mathbf{D_0^2 q_1 + \omega_0^2 q_1 = 0} \tag{21}$$

$$\mathbf{D_0^2 q_2 + 2D_0 D_1 q_1 + k_2 q_1^2 + \omega_0^2 q_2 = 0} \tag{22}$$

$$\mathbf{D_0^2 q_3 + 2D_0 D_1 q_2 + 2D_0 D_2 q_1 + D_1^2 q_1 + k_3 q_1^3 + 2k_2 q_1 q_2 + \omega_0^2 q_3 = 0} \tag{23}$$

Solving Eq. (21) reads [24]:

$$\mathbf{q_1 = A(T_1, T_2) e^{i\omega_0 T_0} + CC} \tag{24}$$

where CC denotess complex conjugate. Assuming $A = a_1 e^{i\varphi}$ [24], and solving Eq. (22) gives:

$$q_2 = \frac{A^2 k_2 e^{2i\omega T_0}}{3\omega_0^2} - \frac{2A\bar{A}k_2}{\omega_0^2} + CC \tag{25}$$

$$\boldsymbol{\varphi = \varphi_0(T_0)}$$
$$\mathbf{a_1 = a_1(T_2)} \tag{26}$$

Solving Eq. (23) results in:

$$\mathbf{q_3 = \frac{A^3 k_2^2 e^{3i\omega T_0}}{12\omega_0^4} - \frac{A^3 k_3 e^{3i\omega T_0}}{8\omega_0^2} + CC} \tag{27}$$

$$\mathbf{a_1 = cte}$$
$$\boldsymbol{\varphi = \left(\frac{3a_1^2 k_3}{8\omega_0} - \frac{a_1^3 k_2^2}{2\omega_0^3}\right) T_2 + \chi} \tag{28}$$

where χ is a constant [24]. It is important to mention that the terms proportional to $e^{i\omega T_0}$ and $e^{-i\omega T_0}$ in the solution of equations (22) and (23) would produce secular terms in the particular solution of q_2 and q_3. Thus, for a uniform expansion, each of the coefficients of $e^{i\omega T_0}$ and $e^{-i\omega T_0}$ must vanish. Putting these coefficients equal to zero would give some equations, since our aim is obtaining the time response equation of the system and solving these equations is not necessary for that, they would not be solved [24].

Substituting equations (24), (25) and (27) in equation (20) and using $\xi = \epsilon q$, the time response equation is obtained as [23]:

$$\boldsymbol{\xi = -\frac{b^2}{2}\left(\frac{k_2}{\omega_0^2}\right) + b\cos(\omega_0 t + \varphi) + \frac{b^2}{6}\left(\frac{k_2}{\omega_0^2}\right)\cos 2(\omega_0 t + \varphi) + \left(\frac{b^3}{48}\left(\frac{k_2^2}{\omega_0^4}\right) + \frac{b^3}{48}\left(\frac{k_3}{\omega_0^2}\right)\right)\cos 3(\omega_0 t + \varphi)} \tag{29}$$

4. Results

In order to show the results of the time response equation, assume a=1, L=1m, the fiber and the matrix made by aluminum and rubber with mechanical properties according to Table 1.

Table 1. Properties of the rubber and the aluminium [25].

Material	$\rho\ (kg/m^3)$	E(pa)	V
Matrix (rubber)	1.1×10^7	1×10^7	0.6
Fiber (aluminum)	2.7×10^3	6.91×10^{10}	0.4

Applying properties represented in Table 1 into equations (1) and (2) gives:

$$E_{eq} = 2.76 \times 10^{10} \text{pa} \tag{30}$$

$$\rho_{eq} = 6.6 \times 10^{6} \frac{\text{kg}}{\text{m}^3} \tag{31}$$

Initial conditions of the cable are assumed to be:

$$\xi = 0 \quad \text{at} \quad t = 0 \tag{32}$$

$$\dot{\xi} = 10 \frac{\text{m}}{\text{s}} \quad \text{at} \quad t = 0 \tag{33}$$

Using equations (29), (32) and (33), the time response diagram of the cable in the vertical direction and for $V_f = 0.4$ and $V_m = 0.6$ is obtained as shown in Fig. 3.

In order to validate the solution obtained by the method of multiple scales that is solved for a cable that is suspended between two fixed supports and materials of aluminum and rubber for the fiber and matrix and length of one meter, it is compared with numerical method of the Runge-Kutta and the result is shown in Fig. 3.

Fig. 3 illustrates that the results of the multiple scales method are in a good agreement with the numerical results of the Runge-Kutta method. Of course, there is a very little difference between the results of these two methods in some points, which is due to the consideration of a limited number of sentences in the expansion of the response in the multiple scales method.

Fig. 4 illustrates that considering $V_f = 0.4$ for aluminum as a reinforcement in the composite cable, causes harmonic time response and a constant amplitude for the vibrational response. It is predicted that the more volume fraction of the matrix, the more nonlinear quadratic and cubic terms in the governing equations of motion effect the vibration of the cable.

In order to investigate the effect of changing the volume fraction of the fiber on the free vibrations of the composite cable, the time response diagram is represented by decreasing the volume fraction of the fiber from $V_f = 0.4$ to $V_f = 0.1$ and applying it into the equations, according to Fig. 5.

Fig. 5 shows that decreasing the volume fraction of the fiber in the composite cable from $V_f = 0.4$ to $V_f = 0.1$ that increased the property of hyperelasticity, causes a nonlinear amplitude of the vibration and the nonharmonic response. Comparing Fig. 3 and Fig. 5, shows that as volume fraction of the rubber increases, the nonlinear terms in the governing equation of the motion significantly effect the time response of the cable.

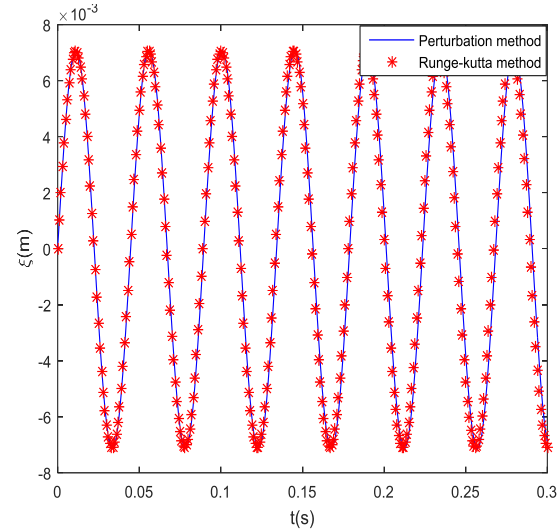

Fig. 3. Validation of the multiple scales solution by comparing it with the Runge-Kutta method

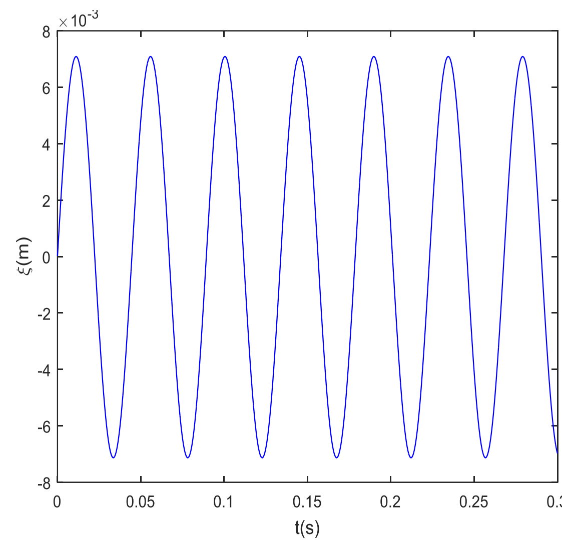

Fig. 4. Time response of the free vibration of the composite cable in the vertical direction for $V_f = 0.4$ and $V_m = 0.6$

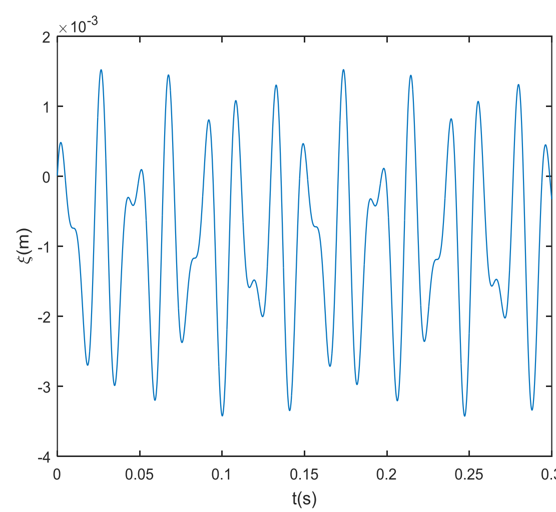

Fig. 5. Time response of the free vibration of the composite cable in the vertical direction for $V_f = 0.1$ and $V_m = 0.9$

Comparing Fig. 4 and Fig. 5 shows the effects of changing in the volume fractions of the fiber and the matrix on the time response of the system. By comparing Figs. 4 and 5, it can be undrestood that increasing the volume fraction of the matrix causes a remarkable decrease in the amplitude of the vibrations. In order to investigate the effect of length of the cable on its vibration, the time response of the system is compared for L=1m and L=3m, when the volume fractions of fiber and matrix are $V_f = 0.4$ and $V_m = 0.6$.

Fig. 6 illustrates that increasing the length of the cable, decreases the amplitude of response which the main reason for that is increasing sag part of the cable that decreases the amplitude of vibration in the vertical direction.

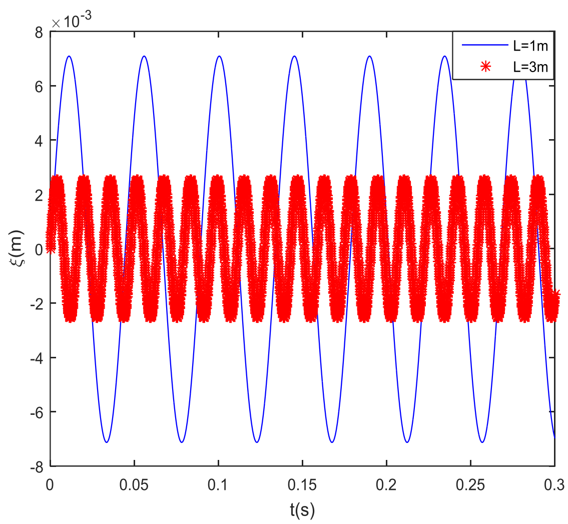

Fig. 6. Comparing the time response of the free vibration of the composite cable in the vertical direction for L=1m and L=3m and when $V_f = 0.4$ and $V_m = 0.6$.

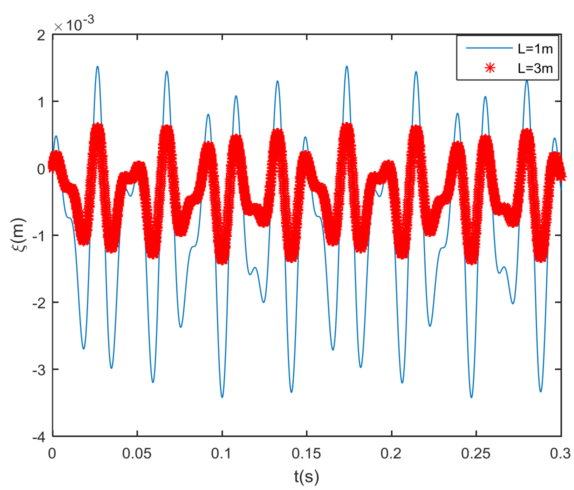

Fig. 7. Comparing the time response of the free vibration of the composite cable in the vertical direction for L=1m and L=3m and when $V_f = 0.1$ and $V_m = 0.9$

The effects of increasing the length of the cable from L=1m to L=3m, when the volume fractions of components of the cable are $V_f = 0.1$ and $V_m = 0.9$ is also investigated in Fig. 7.

Fig. 7 shows that if the length of the cable increases, maximum amplitude of the vibrational cable will decrease even when the matrix volume fraction is much more than fiber in the considered composite cable.

5. Conclusion

In this research, the free vibrations of the composite cable suspended between two fixed supports was studied. Results showed that increasing the volume fraction of the fiber in the composite cable that increased the vibrational properties, caused the time response to be nonharmonic and showed the effects of the quadratic and the cubic nonlinear terms in the governing equation of the motion on the time response diagram. The perturbation method (multiple scales) was compared with Runge-Kutta method and results showed that they were in a good agreement. Effects of length of the cable on its vibration was also investigated.

Nomenclature

ρ	density
E	elasticity modulus
t	time
T	kinetic energy
ε	strain
Π	strain energy
W_{nc}	nonconservative energy
L	length of the cable
P	second Piola Kirchhoff stress
λ & μ	Lamme's Constants
A	cross section of the cable
V	volume fraction
a	Catenary parameter

References

[1] Nayfeh AH, Pai PF. **Linear and Nonlinear Structural Mechanics**. Wiley-Interscience, New York; 2004.

[2] Rega G, Srinil N. Nonlinear Hybrid-Mode Resonant Forced Oscillations of Sagged Inclined Cables at Avoidances. *Journal of computational and nonlinear dynamics* 2007; 2(4): 324-336.

[3] Wang LH, Zhao YY. Non-linear planar dynamics of suspended cables investigated by the continuation technique. *Engineering Structures* 2007; 29(6): 1135-44.

[4] Chen LQ, Ding H. Two nonlinear models of a transversely vibrating string. *Archive of Applied Mechanics* 2008; 78(5): 321-328.

[5] Chen LQ, Zhang W, Zu J. Nonlinear dynamics for transverse motion of axially moving strings. Chaos, *Solitons & Fractals* 2009; 40(1): 78-90.

[6] Rega G. theoretical and experimental nonlinear vibrations of sagged elastic cables. *Nonlinear Dynamic Phenomena in Mechanics* 2012; 181: 159–210.

[7] Salehi AM, Shooshtari A, Esmaeili V, Naghavi A. Nonlinear analysis of cable structures under general loadings. *Finite elements in analysis and design* 2013; 73: 11-19.

[8] Arena A, Pacitti A, Lacarbonara W. Nonlinear response of elastic cables with flexural-torsional stiffness. *International journal of solids and structures* 2016; 87: 267-277.

[9] Yashavanta Kumar GA, Satish Kumar KM. Free vibration analysis of smart composite beam. *Materials today: proceedings* 2017; 4(2): 2487-2491.

[10] Kumar A, Singha MK, Tiwari V. Nonlinear bending and vibration analyses of quadrilateral composite plates. *Thin-Walled Structures* 2017; 113: 170-180.

[11] Piraccini M, Di Sante R. Measurement of nonlinear vibration response in aerospace composite blades using pulsed airflow excitation. *Measurement* 2018; 130: 422-434.

[12] Wang ZX, Shen H. Nonlinear vibration of sandwich plates with FG-GRC face sheets in thermal environments. *Composite structures* 2018; 192: 642-653.

[13] Mao JJ, Zhang W. Linear and nonlinear free and forced vibrations of graphene reinforced piezoelectric composite plate under external voltage excitation. *Composite structures* 2018; 203: 551-565.

[14] Zhang YF, Zhang W, Yao ZG. Analysis on nonlinear vibrations near internal resonances of a composite laminated piezoelectric rectangular plate. *Engineering Structures* 2018; 173: 89-106.

[15] Sheng GG, Wang X. Nonlinear vibration of FG beams subjected to parametric and external excitations. *European journal of mechanics-A\Solids* 2018; 71: 224-234.

[16] Tang Y, Lv X, Yang T. Bi-directional functionally graded beams: asymmetric modes and nonlinear free vibration. *Composites part B: Engineering* 2019; 156: 319-331.

[17] Wang Y, Xie K, Fu T, Shi C. Vibration response of a functionally graded graphene nanoplatelet reinforced composite beam under two successive moving masses. *Composite structures* 2019; 209: 928-939.

[18] Fan Y, Xiang Y, Shen HS. Nonlinear forced vibration of FG-GRC laminated plates resting on visco-Pasternak foundations. *Composite structures* 2019; 209: 443-452.

[19] Liu L, Li J-M, Kardomateas G. Nonlinear vibration of a composite plate to harmonic excitation with initial geometric imperfection in thermal environments. *Composite structures* 2019; 209: 401-423.

[20] Bayat Y, EkhteraeiToussi H. A nonlinear study on structural damping of SMA hybrid composite beam. *Thin-Walled Structures* 2019; 134: 18-28.

[21] Jones R. **Mechanics of composite materials**. Hemisphere Pub. Co., New York; 1975.

[22] Lai WM, Rubin D, Krempl E, **Introduction to continuum mechanics**. Pergamon Press, New York; 1978.

[23] Nayfeh AH. **Perturbation methods**. John Wiley & Sons; 2008.

[24] Nayfeh AH, Mook DT. **Nonlinear Oscillations**. John Wiley & Sons; 2008.

[25] Jones DRH, Ashby MF. **Engineering materials 2: an introduction to microstructures, processing and design**. Elsevier; 2005.